Journal of South American Earth Sciences 124 (2023) 104260

Contents lists available at ScienceDirect

Journal of South American Earth Sciences

journal homepage: www.elsevier.com/locate/jsames

Structure and seismogenic activity of the broken foreland to the south of the Chilean-Pampean flat subduction zone: The San Rafael Block

Julián Olivar [a,b,*], Silvina Nacif [c], Mario Giménez [c], Benjamin Heit [d], Lucas Fennell [a,b], Andrés Folguera [a,b]

[a] Universidad de Buenos Aires, Facultad de Ciencias Exactas y Naturales, Buenos Aires, Argentina
[b] CONICET-Universidad de Buenos Aires, Instituto de Estudios Andinos "Don Pablo Groeber" (IDEAN), Buenos Aires, Argentina
[c] CONICET, Instituto Geofísico-Sismológico 'Ing. F.S, Volponi' (IGSV), Rivadavia, Provincia de San Juan, Argentina
[d] Deutsches GeoForschungsZentrum GFZ, Potsdam, Germany

ARTICLE INFO

Keywords:
Broken foreland
Southern Central Andes
Crustal seismicity
Basement uplift
San Rafael Block
Crustal structure

ABSTRACT

Andean broken foreland zones, located to the east of the highest Andes, are associated with populated areas and sedimentary basins with relative economic importance. Understanding their seismogenic potential is crucial for urban development and infrastructure planning. In particular, the San Rafael Block is part of the broken foreland developed to the south of the Chilean-Pampean flat subduction zone. A local seismic network allows analyzing the seismogenic potential of the San Rafael Block. Earthquake distribution suggests a northeast-dipping ramp rooting at the lower crust, cropping out at the western topographic front of the basement uplift. Gravity data confirm the asymmetry of the San Rafael block with a western topographic front associated with the main structure that exhumes the basement. Seismological and gravity data allow proposing a west-verging structure, contrary to previous interpretations based on surficial structural data. The results presented here identify the highest shallow seismogenic potential on the western side of the block, near the El Nihuil dam, and only deep events at the eastern neotectonic front which allegedly hosted historical earthquake occurrences such as the Villa Atuel-Las Malvinas earthquake in 1929.

1. Introduction

The San Rafael Block is a set of pre-Jurassic basement rocks exhumed in the foreland of the Southern Central Andes, at around 35°S (Criado Roque, 1972; Cingolani et al., 2003). It is located to the south of the Chilean-Pampean flat subduction zone, considerably separated from the Sierras Pampeanas to the north, a broad broken foreland system linked to the flat slab configuration (Fig. 1). The basement block origin has been associated with another hypothetic shallow subduction configuration, the Payenia shallow subduction zone, developed from 13 Ma to 4 Ma (Kay et al., 2006). However, its eastern orogenic front is still associated with contractional neotectonic deformations along the Cerro Negro-Las Malvinas fault, and seismic activity which includes a historical Mw 6.5 event which took place in 1929, known as the Villa Atuel-Las Malvinas earthquake (Fig. 1) (Bastías et al., 1993; Costa et al., 2004, 2006; Folguera et al., 2009; Branellec et al., 2016a; 2016b).

The San Rafael Block was interpreted as a topographic range uplifted by the progressive Andean orogeny propagated from west to east, with an eastward vergence based on mapping of major exposed structures (Ramos and Folguera, 2011; Ramos et al., 2014; Branellec et al., 2016b). These models, however, were not supported by geophysical data. Recent studies in the area made use of gravity and magnetic data in order to trace patterns associated to the structural grain of the basement and its influence on Quaternary magmatism (Richarte et al., 2018; Morales Volosín et al., 2022). Seismicity studies have focused on events with a depth greater than 50 km (i.e., below the crust) (Lupari et al., 2015). Thus, the analysis of the deep crustal structure of the San Rafael Block based on the information that can be extracted from crustal seismicity is still an unexplored topic.

Varied examples of thick-skinned structures developed in the foreland show that these can acquire different vergence and orientation, even opposed to the neighboring mountain range. Some of these examples include the Laramide ranges in the Rocky Mountains of North America (Smithson et al., 1978; Stone et al., 1993; DeCelles, 2004; Yonkee and Weil, 2015), and the Sierras Pampeanas developed over the Chilean-Pampean flat slab subduction segment (González Bonorino,

* Corresponding author. Intendente Güiraldes 2160, Ciudad Universitaria - Pabellón II, C1428EGA – CABA, Argentina.
E-mail address: olivar@gl.fcen.uba.ar (J. Olivar).

https://doi.org/10.1016/j.jsames.2023.104260
Received 2 December 2022; Received in revised form 10 February 2023; Accepted 13 February 2023
Available online 15 February 2023

1950; Jordan and Allmendinger, 1986; Introcaso et al., 1987; Ramos et al., 2002). In those cases, the deep structure models were supported by geophysical data. A more recent work carried out in the easternmost Sierras Pampeanas, based on focal mechanisms and structural geology analysis, showed that the major and medium scale structures of that broken foreland are controlled by the complex structural grain of the basement (Vicente et al., 2022). Similarly, the San Rafael Block region presents a complex history that has imprinted a NW-SE structural grain onto the basement (see geological setting for more details). Here, the lack of geophysical evidence to constrain the deep structure of the block, and the fact that foreland uplift behavior can be strongly controlled by the inherited structural grain, challenge the traditional models that display a N–S structure with eastward vergence in line with the Andes. This motivates the revision of such models using geophysical data and makes this a good case study to contribute knowledge about uplifts in foreland thick-skinned deformation scenarios.

This work conjugates seismological data gathered with a local network and gravity data to show that, even though neotectonics has been described in the eastern topographic front of the San Rafael Block and isolated localities along its axial zone, its deep crustal structure is

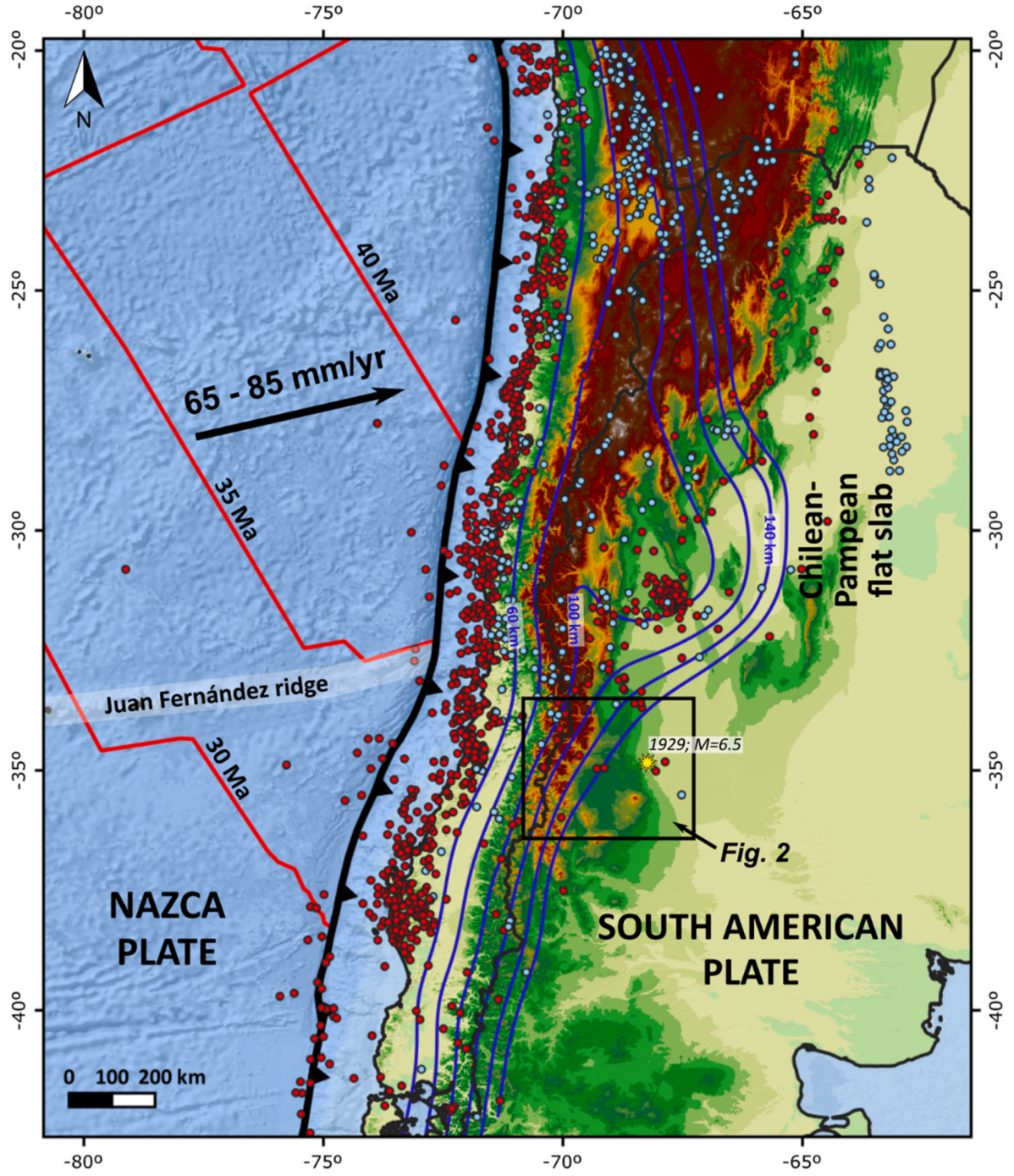

Fig. 1. Seismotectonic setting of the study area. Red lines indicate ocean floor ages (Müller et al., 2016). Blue contours show the depth of the Nazca subducted plate (from Slab2 model, Hayes et al., 2018). Red and light-blue dots represent M > 5.5 seismicity with depth <50 km and >50 km, respectively, from the ISC-GEM catalog (version 6.0, International Seismological Centre, 2019; see also Bondár et al., 2015). The yellow star indicates the approximate location of the historic Villa Atuel-Las Malvinas earthquake.

better explained by a model with westward vergence, contrary to previous models. This determination has important implications in terms of seismological hazard, and urban and infrastructure planning.

2. Geological and tectonic setting

Five morphostructural domains characterize the eastern Andean slope at the latitudes south of the Chilean-Pampean flat subduction zone (Figs. 1 and 2). From west to east, these are the Principal Cordillera, the Frontal Cordillera, and the foreland region comprising the Cerrilladas Pedemontanas, the San Rafael Block and the Payenia volcanic field. Two basins, the Río Grande and Alvear basins, with a Mesozoic to Quaternary infill are flanking the San Rafael Block in the foreland zone isolated from the Andes (Fig. 2). The Principal Cordillera is a hybrid fold and thrust belt characterized by basement uplifts separated by thin-skinned deformational belts (see Fuentes et al., 2016, for a recent synthesis). The Frontal Cordillera is an east-vergent basement block located to the north of Diamante river that exposes pre-Jurassic rocks (Turienzo et al., 2012). The study area is located to the east of these systems, in the foreland area.

The Cerrilladas Pedemontanas are a belt of low hills constituted by folded Neogene strata at surface due to the tectonic inversion of Late Triassic depocenters at depth (Chiaramonte et al., 2000; Cortes et al., 2006; Ahumada and Costa, 2009). This deformational belt is bounded to the east by the La Ventana neotectonic thrust, which folds and cuts Neogene and Quaternary sequences with a dip angle of 30–45° to the west (García and Casa, 2015; García et al., 2015) (Fig. 3). Based on surface structural data, its decollement has been proposed at a depth of 13 km. Mean uplift rates for the Quaternary and the last 150 ka have been estimated at 0.73 mm/year and 1.33 mm/year respectively (García et al., 2015).

The San Rafael Block constitutes a broken foreland system developed 100 km to the east of the Andean front. Pre-Jurassic rocks are exposed between 34.2° and 35.5°S through a NW-SE stripe north of the Atuel river that rotates to a N–S strike to the south (Figs. 2 and 3). The oldest rocks exposed in the San Rafael Block are isolated outcrops of Meso-Proterozoic metamorphic rocks (Cingolani and Varela, 1999; Cingolani et al., 2005; Abre et al., 2011). These rocks correlate with basement rocks exposed in the eastern Sierras Pampeanas broken foreland and, to the south, with the ones exposed in the Las Matras Block in La Pampa province (Cingolani and Ramos, 2017). Unconformably, Ordovician to Devonian marine sequences metamorphosed in the Late Devonian rest on the Precambrian basement (Abre et al., 2017; Tickyj et al., 2017). On top of them, Carboniferous glacial-related marine sequences are unconformably exposed (Dessanti, 1956; Rocha Campos et al., 2011; Henry et al., 2014). Next, Permian to Triassic volcanic rocks of the Choiyoi Group and equivalents crop out in the study region, associated with the extensional destabilization of the western Pangea supercontinent (Mpodozis and Kay, 1990; Llambías et al., 1993; Kleiman and Japas, 2005; Rocha Campos et al., 2006). Finally, scarce Lower Miocene sedimentary rocks of the Aisol Formation unconformably cover the Paleozoic and Triassic units and are interpreted as part of the distal section of

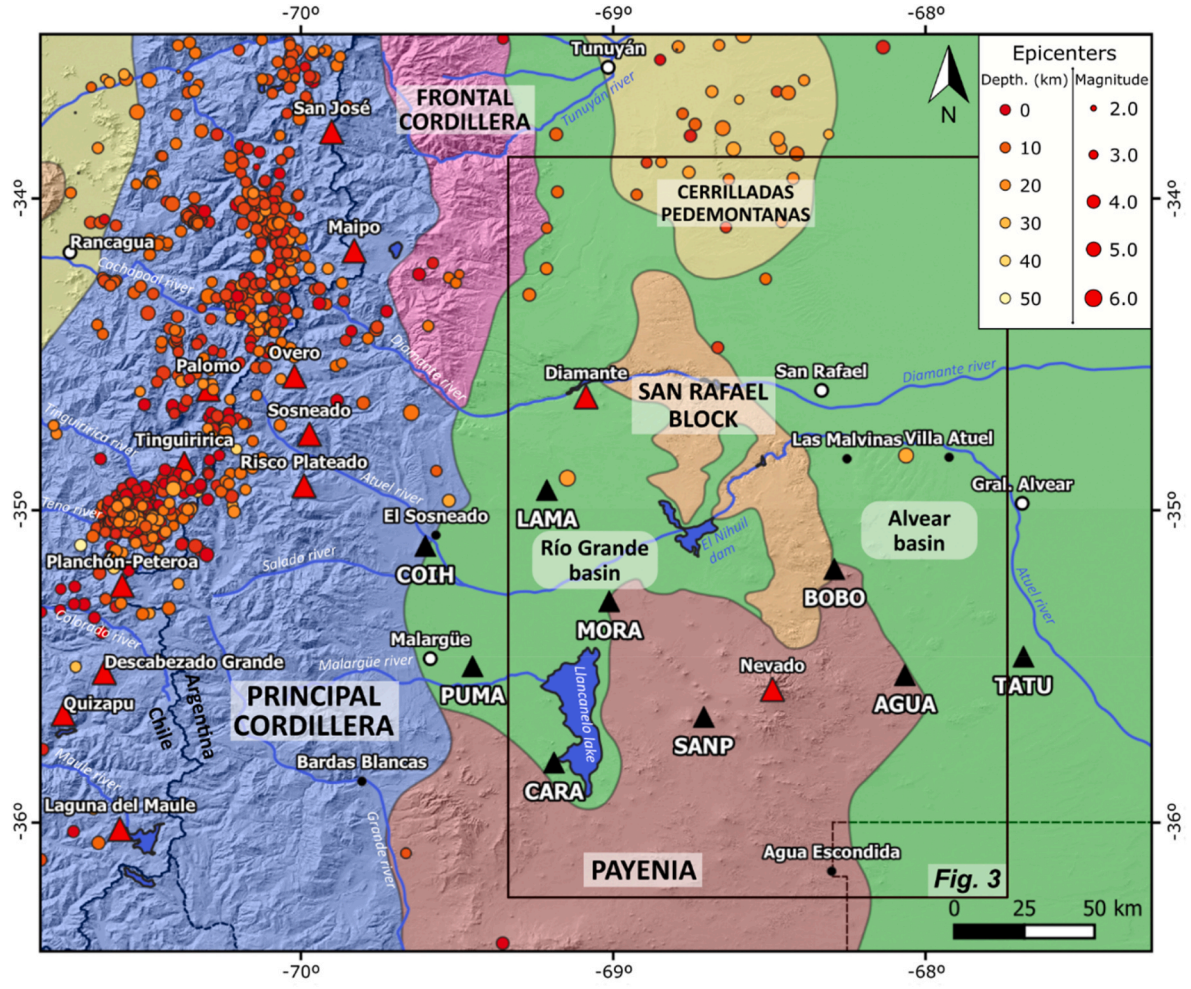

Fig. 2. Morphostructural units, seismological network (black triangles), and crustal seismicity (depth <50 km) from the ISC Reviewed catalog (1980–2022). Only records with location error less than 10 km in every direction are shown. Red triangles correspond to volcanic centers.

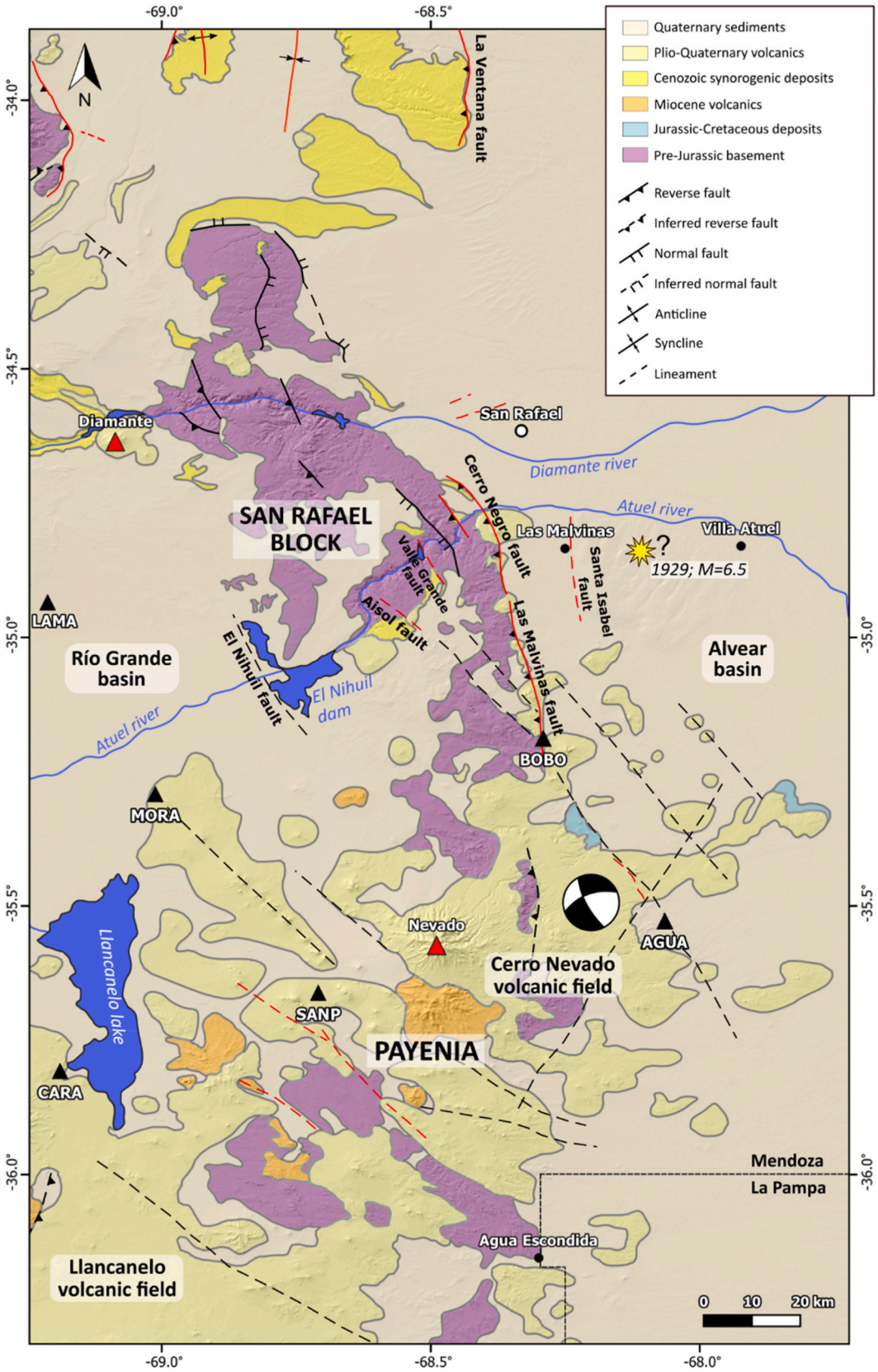

Fig. 3. Simplified geological map of the study area (based on Nullo et al., 2005; Sruoga et al., 2005; Sepúlveda et al., 2007a, 2007b; SEGEMAR, 2021). Structures with red streak indicate Quaternary activity. The yellow star indicates the approximate location of the historic Villa Atuel-Las Malvinas earthquake (exact epicenter is unknown). Focal mechanism taken from the GCMT catalog (Global Centroid Moment Tensor, Dziewonski et al., 1981; Ekström et al., 2012). Note that the San Rafael Block has been interpreted as a mainly eastern vergence-basement structure associated with the Cerro Negro-Las Malvinas eastern fault, where neotectonic activity is concentrated (Bastías et al., 1993).

the Río Grande synorogenic basin cannibalized after the uplift of the San Rafael Block (González Díaz, 1972; Forasiepi et al., 2011).

The San Rafael Block uplift has been associated with a shallow subduction episode occurred in late Miocene times (Kay et al., 2006). During the Pliocene, the San Rafael flat slab segment collapsed and led to widespread retroarc magmatism (Kay et al., 2006; Ramos and Folguera, 2011; Ramos et al., 2014), and, on the western side of the block, NW trending normal faults affecting Miocene sediments (Folguera et al., 2009). However, the retroarc zone still registers tectonic and seismic activity (Cortes et al., 2006; Ahumada and Costa, 2009), as well as Holocene volcanism (May et al., 2018). Even though some authors concluded that the retroarc is subject to an ongoing generalized extension (Ramos and Folguera, 2005; Ramos and Kay, 2006; Folguera et al., 2009), more recent studies lean towards ongoing shortening (Messager et al., 2014; Sagripanti et al., 2015; Branellec et al., 2016a; 2016b; Colavitto et al., 2019). The neotectonic activity in the retroarc zone can be justified based on the transitional geometry between the flat slab to the north and a steep zone to the south (Fig. 1) (Nacif et al., 2015). On the other hand, the widespread Quaternary volcanism in the Payenia Volcanic Province has been associated with an asthenospheric anomaly visualized in a magnetotelluric survey (Burd et al., 2014).

The structure of the San Rafael Block is characterized by NNW to NW structures affecting the different Paleozoic-Mesozoic units conditioned by a lower Paleozoic ductile fabric, derived from the Early Paleozoic deformation and the inversion of the Triassic rift systems (Folguera et al., 2009; Branellec et al., 2016b; Richarte et al., 2018; Morales Volosín et al., 2022). The general vergence of the San Rafael Block has been determined to the east based on the description of neotectonic deformation focused on the eastern topographic flank (Bastías et al., 1993; Costa et al., 2004, 2006; Folguera et al., 2009; Branellec et al., 2016a; 2016b).

Evidence of neotectonic activity has been described in different fault segments within the San Rafael Block and surrounding areas (Fig. 3). Among the basement outcrops lie the Aisol fault (Lucero and Paredes, 1999; Costa y Costa and Cisneros, 2001) and the Valle Grande fault (Costa y Costa and Cisneros, 2001; Peñalva and Velez, 2005), which feature a straight morphology, NW-SE strike, downthrown blocks on the SW side, and descriptions of scarps with Quaternary displacement. To the east of the San Rafael Block the Santa Isabel fault is found, with a N–S strike, downthrown block to the west, and a minimum displacement age of 250 ka based on the dating of pedogenic carbonates affected by the fault (Neilson, 2007). However, the most relevant descriptions of neotectonics are situated in the eastern front of the San Rafael Block, specifically in the Las Malvinas and Cerro Negro faults. Branellec et al. (2016a) argued that these are the only faults in the block that show clear neotectonic morphologic features. They confirmed Pleistocene activity with cosmogenic dating of terraces in the hanging wall (60–80 ka) and assigned them as possible seismogenic structures of the 1929 historic earthquake (M ~6.5), as it had been suggested by previous authors (Bastías et al., 1993; Costa et al., 2006). They proposed that, given the NW-SE to NNW-SSE structural grain, these faults accommodate the shortening component of the E-W stress, while a left-lateral component is hosted by the more linear Aisol and Valle Grande faults.

Even though seismicity is present in the area, catalog records are scarce and previous studies have not attempted to relate it to faulting or volcanism. This question is better approached with the use of local networks as described in the next section.

3. Methodology and results

3.1. Seismic data

We used one year of continuous seismological data available form a local temporary network, from May 2013 to April 2014. Part of this data was processed and published in a previous study along the Andean belt region (Olivar et al., 2022). The seismological experiment was called "Bloque San Rafael" (BSR) and consisted of broadband and short-period stations installed in the vicinities of San Rafael and Malargüe cities (Fig. 2). Only two of the stations ("SANP, "AGUA") had broadband seismometers (Guralp 40 T), another ("PUMA") had 3 short-period sensors, while the rest were equipped with short period 1-component sensors (Teledyne Geotech S13).

Continuous records were manually inspected with SEISAN's Multi Trace View (Havskov et al., 2020) in search for P and S wave arrivals. Phase picking was done manually, given that the events had low magnitudes, which imply low signal to noise ratios hard to tackle with automatic methods. We used a velocity model taken from Lupari et al. (2015) (Table 1). A preliminary localization done using the HYPOCENTER iterative software (Lienert and Havskov, 1995) yielded 133 solutions with depth <50 km inside the study area. During this process, waveforms were manually revised in search for doubtful picks with high residuals and lower weights were assigned to them. Local magnitude was calculated using SEISAN's AUTOMAG routine, which draws local magnitude from the maximum amplitude of the S wave after applying a Wood-Anderson filter. In most cases, results from three to four stations were averaged to obtain the final local magnitude.

Seismic stations were not distributed evenly around the San Rafael Block. In its northern region stations are absent, which leads to high azimuthal gaps in the epicenters located there. This usually means higher uncertainties in the solutions, and thus, harder interpretation of the results. In order to achieve a better assessment of the quality of the locations, we relocated the events using the NonLinLoc software (Lomax et al., 2000; see Appendix for more details). This software carries out a nonlinear nested grid-search, based on the probabilistic formulation of inverse problems (Tarantola and Valette, 1982), which provides a complete probability density function for the hypocenter allowing a more detailed analysis of the quality of the solution and its uncertainties. The program returns a best solution and a 68% confidence ellipsoid calculated from the probability density function. Results were filtered according to the maximum probability parameter (Pmax) among other factors (Pmax >0.01; RMS <0.5 s; distance to the nearest station <125 km; minimum number of phases = 5). This process yielded 89 final locations (see details in Appendix).

Regarding data from other sources, we did not count with many possibilities. Events present in the area according to the ISC Reviewed catalog, for example, are almost null (Fig. 2). On the other hand, the local seismology agency (INPRES) counts with only one short period station in the region, and their database does not report hypocentral errors. Other results derived from the same BSR local network were published by Lupari et al. (2015), corresponding to another time window (December 2011 and May–October 2012). In that study, the HYPOCENTER software was used as the localization method, localizing not only crustal events but also sublithospheric ones. Since the methodology used for filtering their results yielded large errors, in this work we only considered their events with epicentral errors lower than 10 km and depth error lower than 20 km. This selection represents the 77.4% of their dataset with hypocenters above 40 km depth. It is worth mentioning that the events located by those authors do not report

Table 1
Velocity model for the BSR experiment taken from Lupari et al. (2015).

Depth (km)	Vp (km/s)	Vs (km/s)
−5.0	5.522	3.443
0.0	5.711	3.514
5.0	5.843	3.515
20.0	6.353	3.610
35.0	6.811	3.928
45.0	7.245	3.971
55.0	7.473	4.208
90.0	8.034	4.658
120.0	8.779	4.903
210.0	8.829	4.940

magnitudes.

The events located in this work are plotted in Fig. 4, both in plain view and in W-E and N–S sections, with errors shown in 68% confidence ellipses and bars. The average RMS for this group is 0.15 s (σ = 0.07 s), with no locations above 0.3 s. The Pmax parameter is 0.28 (σ = 0.29) in average. Mean latitudinal and longitudinal errors are 2.70 km (σ = 2.07 km) and 2.26 km (σ = 1.08 km), respectively. Average depth error is 6.20 km (σ = 3.05 km), showing that this parameter is the most problematic.

When analyzing the distribution of the different events in plain view, four groups are distinguished. First, north of 34.5°S, to the west, a group of events located between depths of 10 and 30 km are aligned in a 70 km long stripe with NE-SW orientation. In the central area, between 34.5° and 35.3°S, two main groups are distinguishable: to the west of the San Rafael Block, the earthquakes are shallower than 15 km, with eight of them above 5 km depth. These particular events are aligned in a NW direction, following the trace of the El Nihuil fault (Fig. 4), except for three of them located near the "LAMA" station. In that area, the rest of the earthquakes occurred at around 15 km depth. The other group is situated to the east, over the San Rafael Block and eastward. They are

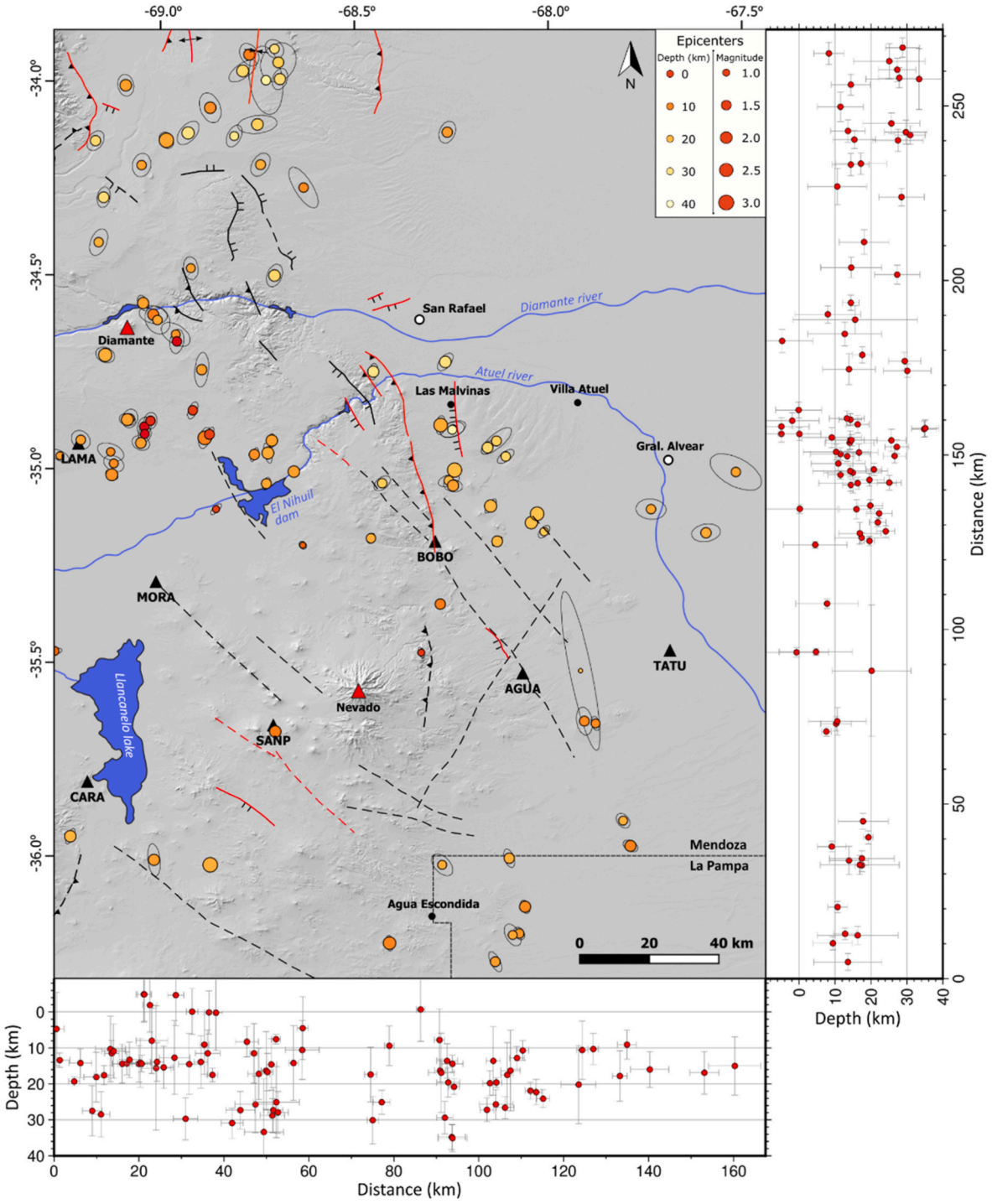

Fig. 4. Locations of the 89 crustal events obtained after applying NonLinLoc and filtering the results, represented in plain view and N–S and E-W sections. Error ellipses and bars indicate Gaussian error with a confidence interval of 68%. Other symbols as in Fig. 3.

deeper than 10 km, reaching occasionally up to 35 km in depth, with an average in the range of 20–30 km. Most of these events are located to the east of the Cerro Negro-Las Malvinas escarpment that defines the eastern topographic front of the San Rafael Block. Finally, to the south, over the Payenia volcanic field, there is a series of disperse earthquakes with depths between 10 and 20 km. In particular, in the surroundings of the Cerro Nevado stratovolcano there is a gap in seismic activity. Most of the events surround the volcanic field, with a radius of more than 50 km from the main edifice.

In cross-section (Fig. 4), distribution of events covers the whole crust, from the surface up to 35 km depth, with an average near 16 km. Some are so shallow that the software locates them above the surface (at 1400 m a.s.l.). That is an error derived from using a grid with search nodes up to 5 km above sea level, and it can be disregarded by looking at the vertical error bars that do reach the surface.

Some of the elements indicated in the description of the plain view are also notorious in the cross-sections (Figs. 4 and 5). In the E-W transect, at 68.5°W, a western shallow group is differentiated from an eastern group which is almost entirely beneath 10 km. In the N–S transect (Fig. 4), the latitudinal division mentioned above also becomes clear, with a group of events that reach the surface in the central sector, and groups of deep disperse events along strike.

Local magnitudes are comprised between 0.8 and 2.8, with an average of 1.6. Only 15 events had magnitudes above 2 (Fig. 5). This explains the absence of most events in the international catalogs, that probably due to the distribution of regional and global networks fail at detecting these low energy events.

The local network is situated in a relatively favorable region with respect to the seismicity being studied. However, azimuthal gaps are still relatively high, with a median at 262°, 86.5% of the events above 200°, and 25.8% above 300°. This directly affects the precision of the hypocentral depth, which, as mentioned before, is the most problematic parameter. Distances of the events to the nearest station have a median at 37.9 km, with 67.4% closer than 55 km (Fig. 5).

Regarding the events located by Lupari et al. (2015) in this region, their distribution follows the tendencies observed in our results. Most of them are located in the central part, at both sides of the San Rafael Block, and are almost absent in the Payenia volcanic field (Fig. 6). These events are deeper than 13 km, most of them lie between 20 and 30 km depth. Errors in average are 3.24 km ($\sigma = 1.84$ km) in latitude, 4.06 km ($\sigma = 2.00$ km) in longitude, and 5.99 km ($\sigma = 3.03$ km) in depth. This is considering, as mentioned before, only the events with epicentral errors under 10 km and vertical error lower than 20 km. Less weight was assigned to these events in our interpretations, since the authors only used the HYPOCENTER software. With our dataset, that software reported overestimated depths in relation to NonLinLoc, so that a direct depth comparison between datasets should be avoided.

3.2. Gravity data

The Bouguer residual anomaly map utilized in this work coincides with a part of the one shown in Richarte et al. (2018) but with a recalculation of the results (Fig. 6B). This is based on the global gravity model EGM2008 (Pavlis et al., 2008, 2012), obtained from terrestrial gravity data and satellite gravity data from GRACE (*Gravity Recovery and Climatic Experiment*), with a spatial resolution of 19 km (Barthelmes, 2009). Richarte et al. (2018) used this model and applied the topographic correction. To do this, the digital elevation model (in their case, ETOPO2) is discretized in spherical prisms of constant density whose gravity effects are added to calculate the total topographic effect (Heck and Seitz, 2007) using a specific software (Álvarez et al., 2012; based on Uieda et al., 2010).

The description of the Bouguer anomaly map yields NW-SE positive values, formed by two smaller-elliptical anomalies, following the western slope of the San Rafael Block (Fig. 6B). Towards the southwest, gravity values diminish more abruptly than towards the northeast. This is observed in the gradient map (Fig. 6C), the gradient is higher on the SW face of the San Rafael Block than in the NE face. Southward, there is an important decrease in gravity values followed by an abrupt increase towards a great positive anomaly in the vicinities of the Cerro Nevado, that shows the maximum values.

We carried out an inversion of the gravity anomaly in search for a density model in depth. For this purpose, we used the 'VOXI' technique (Geosoft), for residual Bouguer data surveys (Elllis et al., 2012; MacLeod and Ellis, 2016). The number of cells (voxels) was set at 155 × 125 voxels and the minimum error at 1 mGal. The reference density for calculation was 2.67 g/cm^3. A 3D grid with densities underneath the San Rafael Block in the first 10 km of the crust was obtained. Fig. 7 shows an E-W transect of this model, where a high density is observed below the block, with an asymmetry displaying an abrupt limit towards the west and a smoother transition to the east.

4. Discussion

In order to carry out a methodical analysis of the seismicity map (Figs. 4 and 5) we can divide the region into three belts: north, central and south from the San Rafael Block.

In the northern area (Fig. 5, top block), the seismic events locate to the east of the Frontal Cordillera, in the transition zone between the southern end of the Cerrilladas Pedemontanas and the northern limit of the San Rafael Block. The seismic activity in the Cerrilladas Pedemontanas is well known, even present in the international catalogs such as the ISC. In this study, we find two groups of events between 10 and 15 km depth and at around 30 km following a NE-SW trend. The first group is compatible with the 13 km deep decollement proposed by previous authors, based on surface data, for the frontal thrust of this system (La Ventana fault, García et al., 2015). The deep group is most likely indicating the presence of a seismogenic source corresponding to a basement structure, maybe delimiting domains with different mechanics in the Cerrilladas Pedemontanas and the San Rafael Block.

In contrast, along the southern region (Fig. 5, bottom block), a lower density of seismic events is found. Particularly, surrounding the Cerro Nevado volcanic center, only two events were registered. The lack of volcanic seismicity is expected due to the absence of historical eruptivity in this volcanic center, with youngest magmatic products at around 1 My (Quidelleur et al., 2009), while the scarcity of tectonic events could be due to a hot crust associated with the Payenia asthenospheric anomaly. The sparse recorded events are possibly associated with NW and NE striking basement structures up to 15 km deep that have been previously identified from magnetic anomalies (Morales Volosín et al., 2022).

The central area holds the majority of the located events (Fig. 5, central block). For this region, we added information provided by gravity data to the discussion. This and the earthquake distribution display some interesting characteristics when compared with current structural models for the San Rafael Block. Previous works noting that Quaternary tectonic activity concentrated mainly on the eastern topographic front along the Cerro Negro-Las Malvinas fault, had interpreted a deep west dipping ramp that became horizontal in a decollement located in the lower crust as the main structure uplifting the block (Folguera et al., 2009; Ramos and Folguera, 2011; Ramos et al., 2014; Branellec et al., 2016b). However, it is worth noting that these schemes were not supported by geophysical information. The data gathered in this study do not favor such model and lead to a new interpretation of the crustal structure. The analysis is aided by a transect perpendicular to the NW-SE structural tendency of the region (A-A′, Figs. 6 and 8), which includes the surface information about ancient and recent structures, geophysical data of the basement structural grain, the orientation of the block's outcrops, and the direction of the elongated gravity anomaly.

First, several seismic epicenters are located to the east of the Cerro Negro-Las Malvinas fault and not over the fault itself or to the west as can be expected for a west-dipping fault (Figs. 6 and 8). These events are deeper than those located to the west side of the San Rafael Block, next

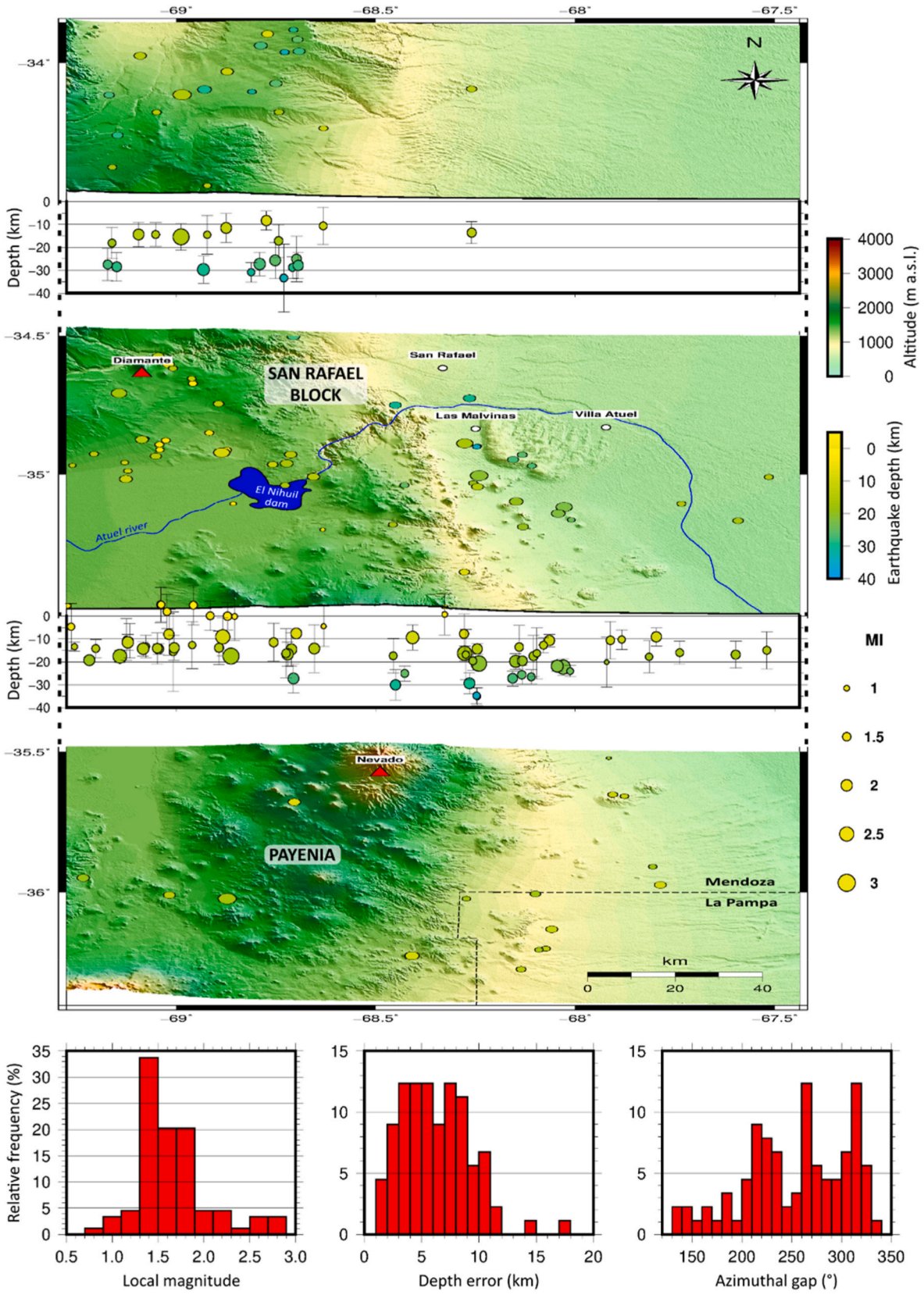

Fig. 5. 3D view of the located events and histograms of three parameters. Earthquakes of the upper block are shown in the upper transect, while those of the other two blocks are projected in the lower section.

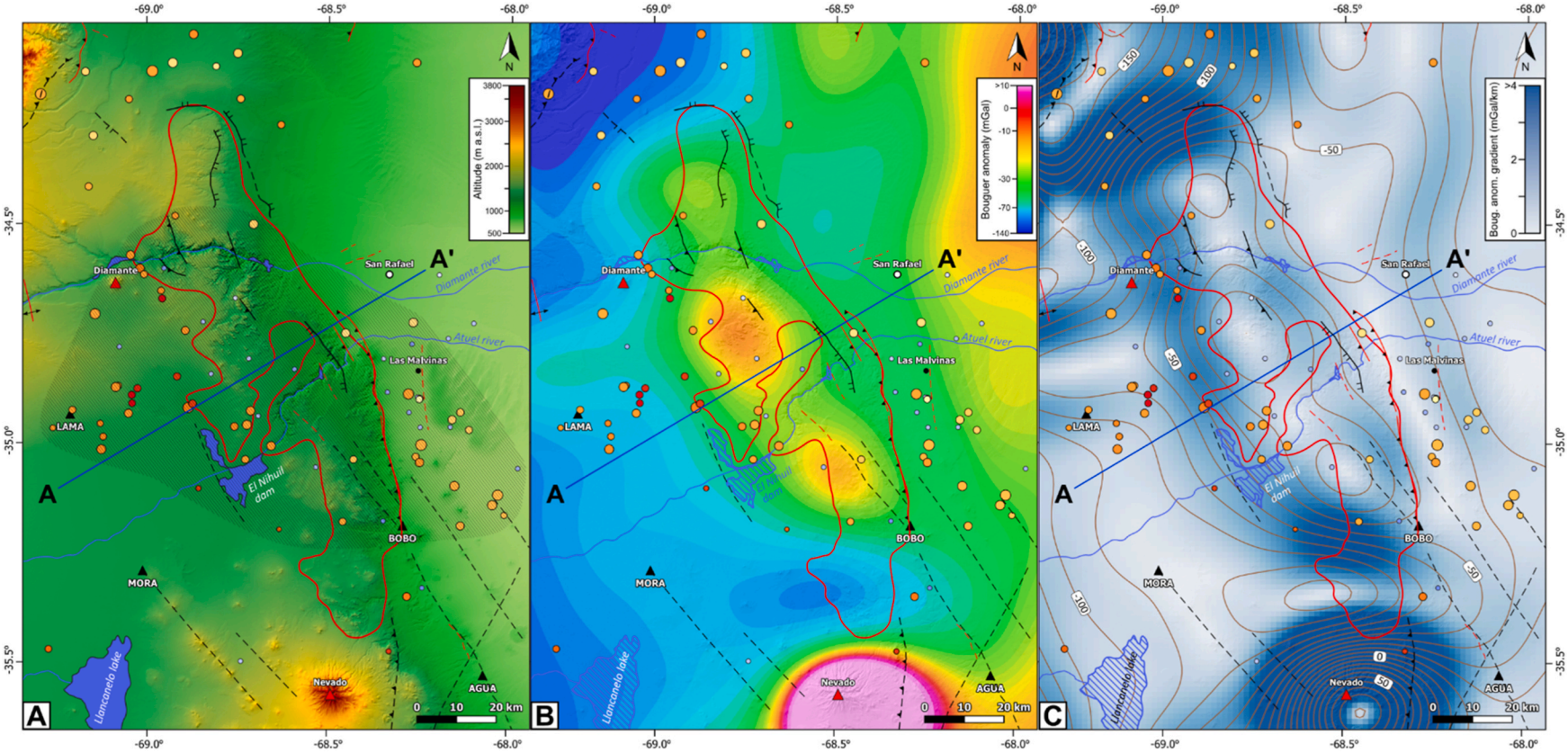

Fig. 6. Crustal seismicity located in the vicinities of the San Rafael Block (red polygon) in this study (range of reds, same representation as in Fig. 4) and by Lupari et al. (2015; range of blues, stronger color indicates shallower depth, unknown magnitude). Blue line indicates the A-A′ section shown in Fig. 8, perpendicular to the NW-SE structural grain of the region. Seismicity is compared to different variables: A) Topography; B) Bouguer residual anomaly; C) Contours and gradient of the Bouguer residual anomaly. Shaded area in A indicates the earthquakes projected in the section. Other symbols as in previous figures.

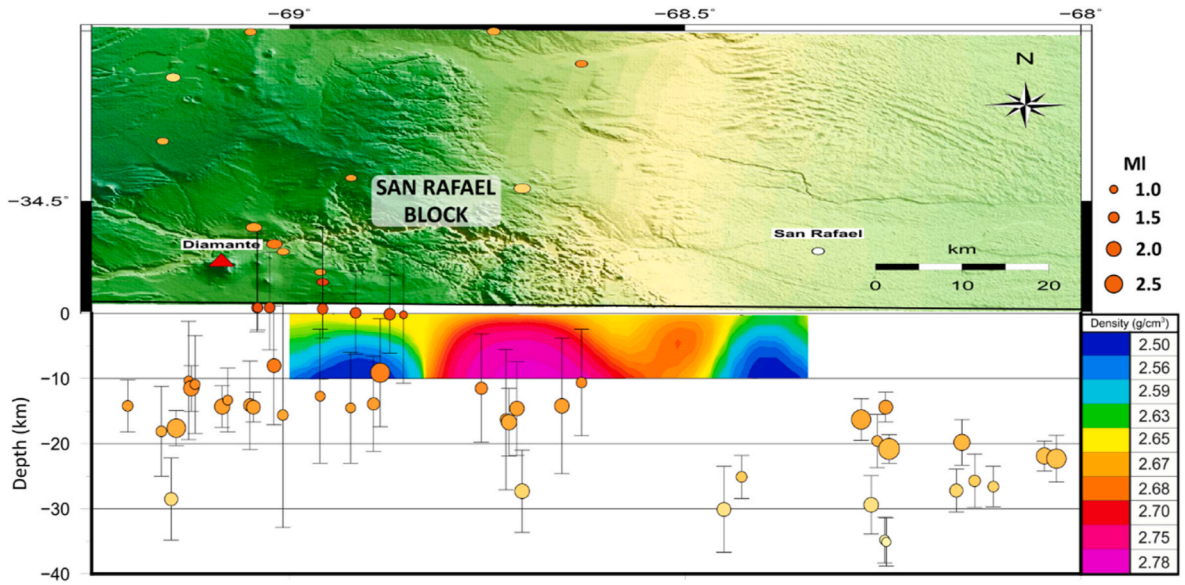

Fig. 7. Inversion of gravity data and seismicity projected to an E-W transect, showing the main density contrast below the San Rafael Block. Note the asymmetry of the high-density region, with an abrupt limit on the west side. Note that this software only allows drawing E-W and N–S transects of the model, so that this section is not perpendicular to the NW-SE structural grain of the region.

to the El Nihuil dam, in some cases reaching depths close to the Moho (according to Heit et al., 2008; Uieda and Barbosa, 2017). The latter is particularly important given that the eastern flank is considered by many authors not only as the main neotectonic structure, but also as the deformation leading edge associated with the exhumation of the San Rafael Block basement structure. There is a progressive deepening of the hypocenters from shallowest in the western side to deepest in the eastern one that could indicate a crustal scale northeast-dipping structure, discussed below in more detail.

The Bouguer anomaly map shows that the positive NW-SE elongated anomaly that matches the San Rafael Block is asymmetric. While the western side of this structure is characterized by a gravity gradient around 2.5 mGal/km, the eastern region reaches only 1.5 mGal/km (Figs. 6 and 8). We interpret these gradients in terms of the contrast of different levels of basement rocks that have increasing densities with depth (according to Richarte et al., 2018). Such contrasts could be produced by structures that displace the basement vertically, introducing a shift in the density stratification. The positive anomaly could be related to the exhumation of deeper basement levels. Then, the higher gravity gradient in the western side would respond to a stronger density contrast generated by a higher displacement of the basement, also cutting through deeper levels than in the eastern side. This implies a more prominent structure thrusting the basement on the west side than on the east. Such interpretation is consistent with a northeast dipping crustal structure indicated by the seismicity distribution. We propose that this is the main structure that uplifts the San Rafael Block, with a minor fault on the eastern front setting up a bi-vergent configuration (Fig. 9). The field evidences of neotectonics found in the east side would be associated to activity in this minor fault. Even though this proposal contradicts previous structural models that suggest an east-vergence and maximum basement exhumation in that direction, it does explain the observed geophysical data. It is also compatible with the density model obtained from the inversion of gravity data (Fig. 7), where an E-W transect shows an abrupt break in the western side of the highest density bulge (dense basement rocks), and a milder transition towards the east.

The topography of the San Rafael Block is also asymmetric, with a steeper and shorter western slope and a more gentle and longer eastern one (Fig. 8). This geometry is easier to explain with the suggested model, where the block would be relatively uplifted in the western side compared to the eastern one if exogenous factors are disregarded (considering the recent age of exhumation; Folguera et al., 2009). The step in altitude observed between the Rio Grande basin (~1300 m a.s.l.) and the Alvear basin (~700 m a.s.l.) (Figs. 6 and 8) could partly be explained by the asymmetric uplift of the block, where the higher southwest side could have served as a topographic barrier for sediments coming from the Andes. This would lead to the filling of the Río Grande basin up to a higher elevation than the Alvear basin, with an abrupt difference between the two instead of a smooth slope throughout the foreland.

The distribution of hypocenters allows two alternative interpretations that do not alter the main proposal substantially (Fig. 9). As mentioned before, these are based mainly in our dataset since the events reported by Lupari et al. (2015) were not reprocessed with NonLinLoc. In both models, the seismicity to the west of the San Rafael Block at nearly 15 km depth was interpreted as related to the main Andean decollement beneath the Río Grande foreland basin that propagates from the Frontal Cordillera. This correlates with the depth of earthquakes reported in that sector in a previous work (Olivar et al., 2022). Beneath the San Rafael Block the main basement ramp interpreted in both models dips to the northeast according to the seismicity. However, beneath 20 km depth, the event distribution is diffuse and allows at least two likely models. One possibility is one major structure that reaches the Moho, spreading into a broader damaged zone (Fig. 9A). An alternative model involves the presence of more than one deep thrust (Fig. 9B), related to structures observed in the surface like the Aisol and Valle Grande faults.

Regionally, it is worth noting that the western end of the main structure introduced in this work coincides with the position of the interpreted suture between the Chilenia and Cuyania terranes (Ramos et al., 1998). Therefore, the earthquake distribution could be reflecting the Andean-neotectonic reactivation of this crustal discontinuity. However, the position and geometry of the suture in this region are not constrained by geophysical evidence in previous works, so that we cannot confirm its connection with the proposed structure.

There are some minor elements of the model that require a brief analysis. The shallowest earthquakes located to the SW of the main thrust were interpreted as a ramification from the major thrust (Fig. 9, blue dotted line), or a minor shortcut fault (red line). The absence of seismicity above 10 km depth on the eastern side of the San Rafael Block impedes any inference about the deep structure of the Cerro Negro-Las

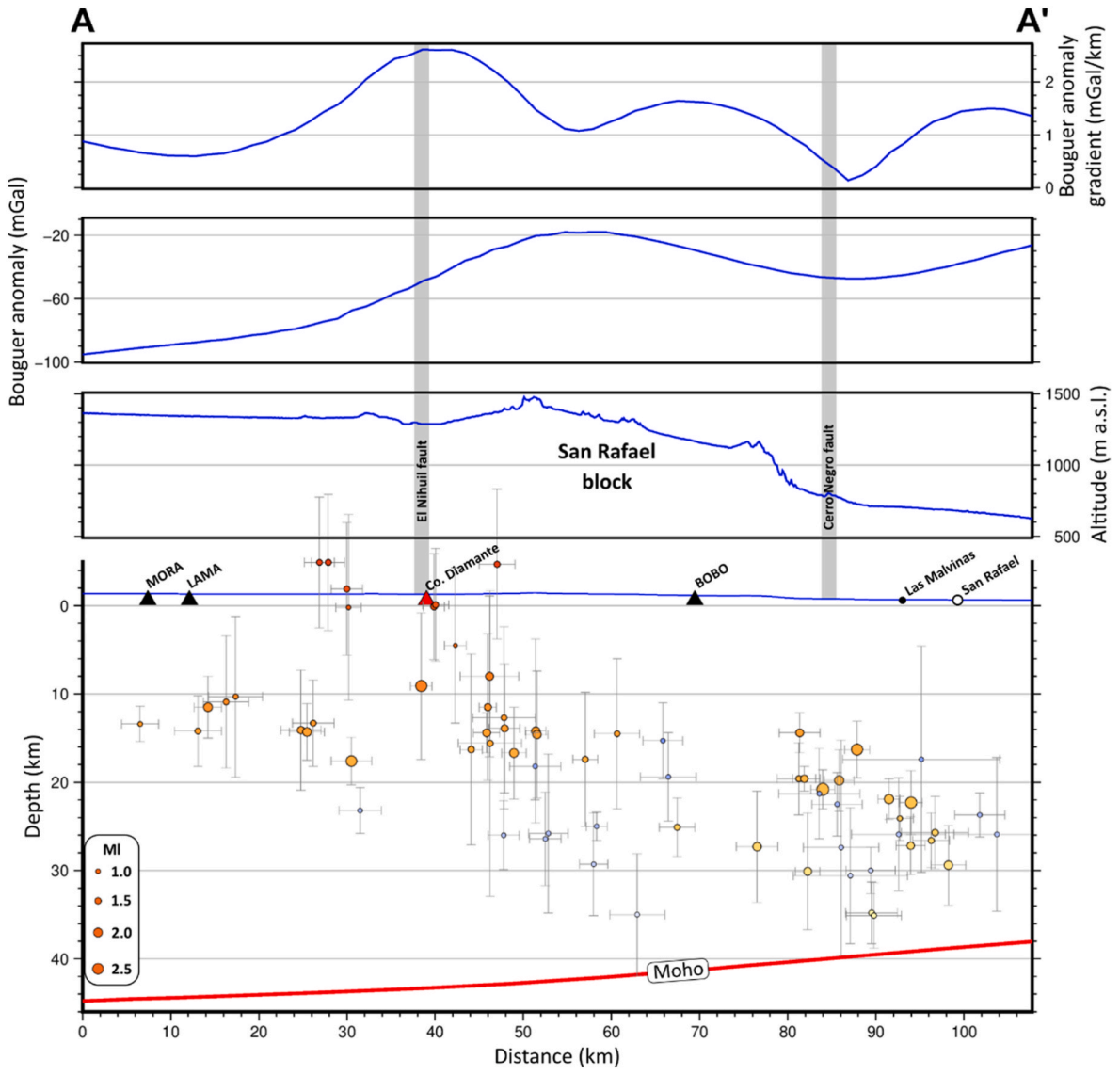

Fig. 8. A-A′ transect (see Fig. 6 for location and projected earthquakes). In the lower section, with the same scale in the horizontal and vertical axes, we project the seismic events from this study (range of reds) and from Lupari et al. (2015; range of blues, unknown magnitude), as well as seismic stations, localities and volcanoes following the same representation as in previous figures. Events are shown with error bars (68% confidence). We also project the Moho (Uieda and Barbosa, 2017) and the topography to scale (blue line). Above, the three sections correspond to the variables shown in the "A" (exaggerated topography), "B", "C" maps from Fig. 6. With gray stripes, as reference, the locations of known structures that limit both sides of the San Rafael Block are shown.

Malvinas neotectonic fault, so that it is drawn schematically (Fig. 9A) or with an estimated depth of 4 km as suggested by Branellec et al. (2016a) (Fig. 9B). The lack of seismicity and smoother Bouguer anomaly gradient suggest a lower fault displacement in relation to the western main fault.

The suggested structure of the San Rafael Block, contrary to previous proposals, is similar to the Sierras Pampeanas broken foreland interpretations, where east-dipping listric ramps rooted in the Moho were proposed with an opposite vergence in relation to the general east-Andean vergence (González Bonorino, 1950; Jordan and Allmendinger, 1986; Ramos et al., 2002; Vicente et al., 2022). In particular, Introcaso et al. (1987) modelled the deep structure of the Sierras de Córdoba (part of the southern Sierras Pampeanas broken foreland) using gravity data, showing that these were uplifted by east-dipping structures rooted in the Moho. Alike this work, in their model the higher positive anomalies are displaced to the west of the main basement structures axial zones, in accordance with a topographic asymmetry of the sierras. The modelled sources are density contrasts hosted in the mid to lower crust. Another example is the Pie de Palo basement structure in San Juan province, that constitutes a west-vergent antiform modelled, based on the earthquake distribution and focal mechanisms, as an east-dipping ramp coupled with a basement wedge at depth (Ramos et al., 2002; Meigs et al., 2006).

Finally, we interpret that the proposed structural model would respond to the structural anisotropies inherited from the basement history and the opening of the Cuyo basin, where the NW-SE strike was imprinted onto the region. We argue that most probably the roughly E-W Andean compression was accommodated by an already NE dipping structure present in the basement, such as the normal faults of the Cuyo basin western limit or eventually the terrane suture.

5. Conclusions

One and a half years of seismic records from a local network located in the Andean foreland zone between 34 and 36.3°S latitude has allowed to produce a map of low magnitude crustal seismic events ($M < 3$). This

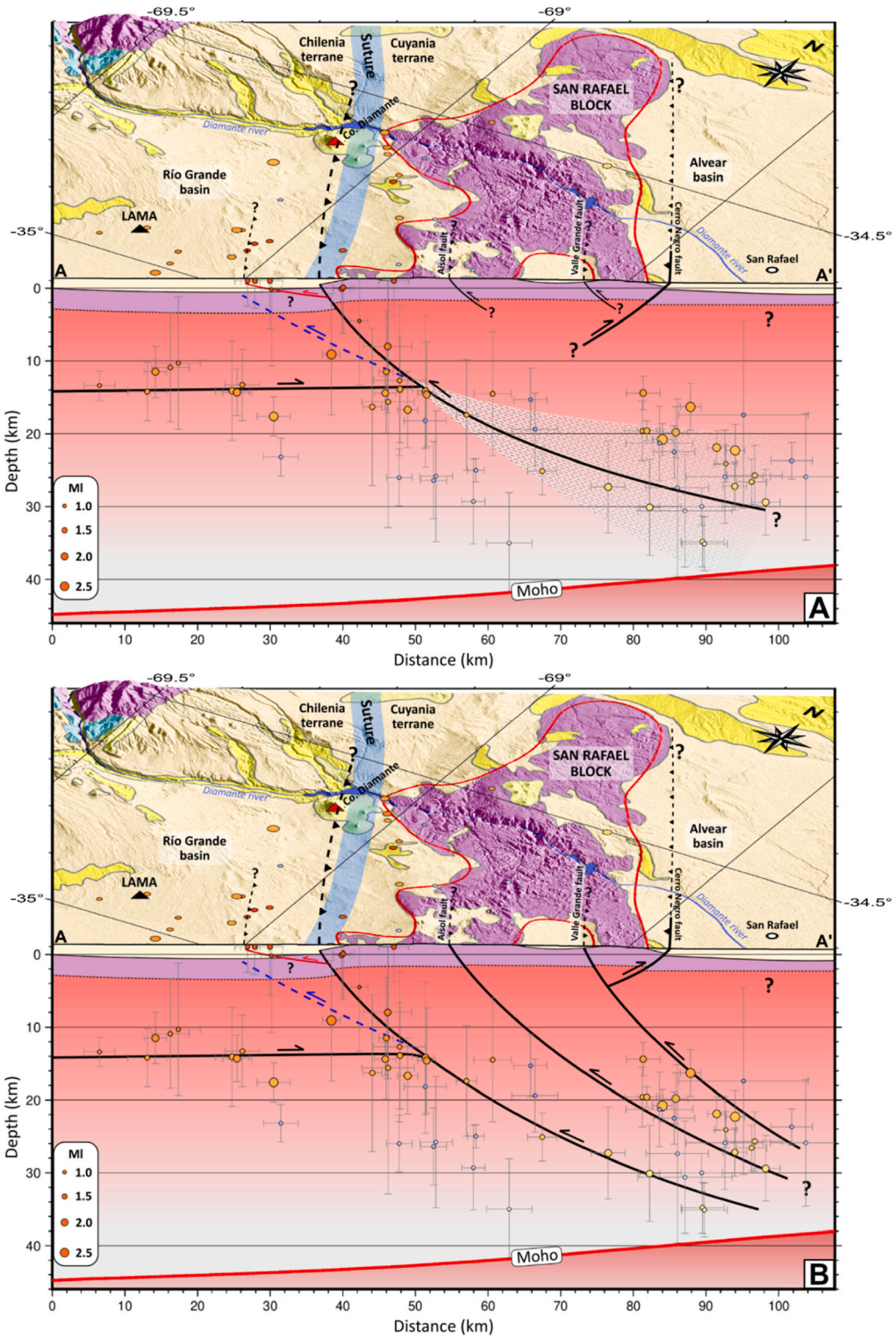

Fig. 9. 3D visual of the geology and deep structure models proposed for the San Rafael Block region (see color code in Fig. 3). Location of the A-A′ transect and the events projected are shown in Fig. 6. Lower section with earthquakes and Moho is the same as in Fig. 8, but plotting the shallowest events beneath the surface. A) The main fault is spread into a fault zone in depth, represented by the shaded cone. B) Alternate geometry in which the main fault is distributed in an imbricate thrust fan.

zone covers the Andean foothills (southern end of the Cerrilladas Pedemontanas), the San Rafael Block, a basement block isolated from the Andes, and the Payenia volcanic field. Most of the crustal seismicity is located in the San Rafael Block and surrounding areas, up to 150 km away from the Andean topographic break. In the Cerrilladas Pedemontanas, seismic events align with a NE-SW orientation and reach only up to 50 km from the Andean front and up to 35 km in depth. To the south, in the Payenia volcanic field, the crustal seismicity is scarce and is almost absent near the Cerro Nevado, one of the major volcanic centers in this region. The only few events are located at around 15 km depth and in regional coincidence with the main faults identified in magnetic and field surveys that have been related in previous works to the main

magmatic paths to the surface.

Seismic and gravity data allow the interpretation of a new model for the San Rafael Block deep structure that had been assumed as controlled by a west dipping crustal ramp in previous works. Seismic events are shallower in the western side of this structure and become progressively deeper to the east, towards the Alvear basin. Additionally, the block shows a higher gravity gradient on the SW slope than on the NE one, following a similar topographic asymmetry. Since the positive gravimetric anomaly is displaced towards the SW slope in relation to the center of the block, high density basement rocks that produce them are inferred to be differentially exhumed in this direction, which is supported by the inversion model. The higher gravity gradient is explained by a greater density contrast as a result of this differential exhumation on the SW side. Therefore, the main and seismically active fault that uplifts the San Rafael Block is presumed to have a NW strike following its topographic expression and the regional structural grain, dipping to the NE, in accordance with the gravity and seismic data. Based on the distribution of hypocenters, this is interpreted as a crustal structure rooted in the Moho that could be related to the inherited structure from the Paleozoic accretional history in the area. Neotectonic structures identified in previous surveys are preferentially located in the eastern topographic front, which in our model constitute lower hierarchy antithetic structures associated with a bi-vergent configuration. Shallower seismicity does not correlate with the site of occurrences of these deformations, indicating that the main seismic hazard would be focused in the western side surrounding the El Nihuil dam. Finally, the suggested structure for the San Rafael Block is similar to other structures in the Pampean broken foreland to the north, associated with east-dipping crustal ramps.

CRediT authorship contribution statement

Julián Olivar: Writing – review & editing, Writing – original draft, Visualization, Supervision, Software, Methodology, Investigation, Formal analysis, Data curation, Conceptualization. **Silvina Nacif:** Writing – review & editing, Validation, Supervision, Resources, Methodology, Funding acquisition. **Mario Giménez:** Visualization, Validation, Software, Resources, Methodology, Funding acquisition, Data curation. **Benjamin Heit:** Writing – review & editing, Validation, Software, Resources, Methodology, Funding acquisition. **Lucas Fennell:** Writing – review & editing, Validation, Investigation, Conceptualization. **Andrés Folguera:** Writing – review & editing, Writing – original draft, Validation, Supervision, Resources, Project administration, Funding acquisition, Formal analysis, Conceptualization.

Declaration of competing interest

The authors declare that they have no known competing financial interests or personal relationships that could have appeared to influence the work reported in this paper.

Data availability

Data will be made available on request.

Acknowledgements

Our research was supported by PICTO N° 254 Seismic Risk through FONCyT 2007 Announcement (CONICET, Argentina). We would like to thank the Pierre Auger Observatory, Malargüe, Argentina; which helped us in the deployment stage and offered their installations for 4 seismological stations of the BSR experiment. This work has also been supported by "Proyecto Unidad Ejecutora IDEAN: Evolución geológica de los Andes y su impacto económico y ambiental". This is the R-448 contribution of the Instituto de Estudios Andinos "Don Pablo Groeber". We also thank Drs. Frederik Tilmann and Xiaohui Yuan of the GFZ (Potsdam, Germany) for providing support, tools, and suggestions to improve the manuscript; and the "StRATEGy" project (GFZ, University of Potsdam, University of Buenos Aires) for providing financial support for the main author's 8-week stay at GFZ in Potsdam. The complete list of seismic events is available in the supporting information (Appendix A).

Appendix A. Supplementary data

Supplementary data to this article can be found online at https://doi.org/10.1016/j.jsames.2023.104260.

References

Abre, P., Cingolani, C., Zimmermann, U., Cairncross, B., Chemale Jr., F., 2011. Provenance of ordovician clastic sequences of the san Rafael block (central Argentina), with emphasis on the ponón trehué formation. Gondwana Res. 19 (1), 275–290. https://doi.org/10.1016/j.gr.2010.05.013.

Abre, P., Cingolani, C.A., Uriz, N.J., Siccardi, A., 2017. Sedimentary provenance analysis of the ordovician ponón trehué formation, san Rafael block, mendoza-Argentina. In: Cingolani (Ed.), Pre-carboniferous Evolution of the San Rafael Block. Springer, Argentina, pp. 59–74 (Cham).

Ahumada, E.A., Costa, C.H., 2009. Antithetic linkage between oblique Quaternary thrusts at the Andean front, Argentine Precordillera. J. S. Am. Earth Sci. 28 (3), 207–216. https://doi.org/10.1016/j.jsames.2009.03.008.

Álvarez, O., Gimenez, M., Braitenberg, C., Folguera, A., 2012. GOCE satellite derived gravity and gravity gradient corrected for topographic effect in the South Central Andes region. Geophys. J. Int. 190 (2), 941–959. https://doi.org/10.1111/j.1365-246X.2012.05556.x.

Barthelmes, F., 2009. Definition of Functionals of the Geopotential and Their Calculation from Spherical Harmonic Models: Theory and Formulas Used by the Calculation Service of the International Centre for Global Earth Models (ICGEM).

Bastías, H., Tello, G., Perucca, L., Paredes, J.D.D., Ramos, V., 1993. Peligro sísmico y neotectónica. In: Ramos (Ed.), Geología de la provincia de Mendoza: XII Congreso Geologico Argentino Relatorio, pp. 645–658.

Bondár, I., Engdahl, E.R., Villaseñor, A., Harris, J., Storchak, D., 2015. ISC-GEM: global instrumental earthquake catalogue (1900–2009), II. Location and seismicity patterns. Phys. Earth Planet. In. 239, 2–13. https://doi.org/10.1016/j.pepi.2014.06.002.

Branellec, M., Niviere, B., Callot, J.P., Regard, V., Ringenbach, J.C., 2016. Evidence of active shortening along the eastern border of the San Rafael basement block: characterization of the seismic source of the Villa Atuel earthquake (1929), Mendoza province, Argentina. Geol. Mag. 153 (5–6), 911–925. https://doi.org/10.1017/S0016756816000194.

Branellec, M., Nivière, B., Callot, J.P., Ringenbach, J.C., 2016. Mechanisms of basin contraction and reactivation in the basement-involved Malargüe fold-and-thrust belt, Central Andes (34–36 S). Geol. Mag. 153 (5–6), 926–944. https://doi.org/10.1017/S0016756816000315.

Burd, A.I., Booker, J.R., Mackie, R., Favetto, A., Pomposiello, M.C., 2014. Three-dimensional electrical conductivity in the mantle beneath the Payún Matrú Volcanic Field in the Andean backarc of Argentina near 36.5 S: Evidence for decapitation of a mantle plume by resurgent upper mantle shear during slab steepening. Geophys. J. Int. 198 (2), 812–827. https://doi.org/10.1093/gji/ggu145.

Chiaramonte, L., Ramos, V.A., Araujo, M., 2000. Estructura y sismotectónica del anticlinal Barrancas, cuenca Cuyana, provincia de Mendoza. Rev. Asoc. Geol. Argent. 55 (4), 309–336.

Cingolani, C.A., Ramos, V.A., 2017. Pre-Carboniferous tectonic evolution of the San Rafael block, Mendoza province. In: Cingolani (Ed.), Pre-carboniferous Evolution of the San Rafael Block. Springer, Argentina, pp. 239–255 (Cham).

Cingolani, C.A., Varela, R., 1999. The San Rafael Block, Mendoza (Argentina): Rb-Sr isotopic age of basement rocks. In: South American Symposium on Isotope Geology, pp. 23–26.

Cingolani, C.A., Manassero, M., Abre, P., 2003. Composition, provenance, and tectonic setting of Ordovician siliciclastic rocks in the San Rafael block: southern extension of the Precordillera crustal fragment, Argentina. J. S. Am. Earth Sci. 16 (1), 91–106. https://doi.org/10.1016/S0895-9811(03)00021-X.

Cingolani, C.A., Llambías, E.J., Basei, M.A.S., Varela, R., Chemale Junior, F., Abre, P., 2005. Greenvillian and Famatinian-age ingneous events in the San Rafael block, Mendoza Province, Argentina: geochemical and isotopic constraints. In: Pankhurst, Veiga (Eds.), Gondwana 12: Geological and Biological Heritage of Gondwana. Academia Nacional de Ciencias, Mendoza, p. 103.

Colavitto, B., Sagripanti, L., Fennell, L., Folguera, A., Costa, C., 2019. Evidence of Quaternary tectonics along Río Grande valley, southern Malargüe fold and thrust belt, Mendoza, Argentina. Geomorphology 346, 106812. https://doi.org/10.1016/j.geomorph.2019.06.025.

Cortes, J.M., Casa, A., Pasini, M., Yamín, M., Terrizano, C., 2006. Fajas oblicuas de deformación neotectónica en Precordillera y Cordillera Frontal (31° 30′-33° 30′ LS): controles paleotectónicos. Rev. Asoc. Geol. Argent. 61 (4), 639–646.

Costa, C., Cisneros, H., 2001. Revisión de la información geológico-estructural del área del Complejo Minero fabril San Rafael.

Costa, C.H., Cisneros, H., Salvarredi, J., Gallucci, A., 2004. Nuevos datos y reconsideraciones sobre la neotectónica del margen oriental del bloque de San

Rafael. 12ª Reunión sobre Microtectónica y Geología Estructural (Cafayate). Resúmenes (7).
Costa, C., Cisneros, H., Salvarredi, J., Gallucci, A., 2006. La neotectónica del margen oriental del bloque de San Rafael: nuevas consideraciones. Asociación Geológica Argentina, Serie D: Publicación Especial 6, 33–40.
Criado Roque, P., 1972. Bloque de San Rafael. In: Leanza, A. (Ed.), Geologia Regional Argentina. Academia Nacional de Ciencias. Córdoba, pp. 283–295.
DeCelles, P.G., 2004. Late Jurassic to Eocene evolution of the Cordilleran thrust belt and foreland basin system, western U.S.A. Am. J. Sci. 304 (2), 105–168. https://doi.org/10.2475/ajs.304.2.105.
Dessanti, R.N., 1956. Descripción Geológica de la Hoja 27c, Cerro Diamante (Provincia de Mendoza). Servicio Nacional Minero Geológico, Boletín 85, 1–79 (Buenos Aires).
Dziewonski, A.M., Chou, T.A., Woodhouse, J.H., 1981. Determination of earthquake source parameters from waveform data for studies of global and regional seismicity. J. Geophys. Res. Solid Earth 86 (B4), 2825–2852. https://doi.org/10.1029/JB086iB04p02825.
Ekström, G., Nettles, M., Dziewoński, A.M., 2012. The global CMT project 2004–2010: Centroid-moment tensors for 13,017 earthquakes. Phys. Earth Planet. In. 200, 1–9. https://doi.org/10.1016/j.pepi.2012.04.002.
Elllis, R.G., de Wet, B., Macleod, I.N., 2012. Inversion of magnetic data from remanent and induced sources. ASEG Extended Abstracts 2012 (1), 1–4. https://doi.org/10.1071/ASEG2012ab117.
Folguera, A., Naranjo, J.A., Orihashi, Y., Sumino, H., Nagao, K., Polanco, E., Ramos, V.A., 2009. Retroarc volcanism in the northern San Rafael Block (34–35 30′ S), southern Central Andes: Occurrence, age, and tectonic setting. J. Volcanol. Geoth. Res. 186 (3–4), 169–185. https://doi.org/10.1016/j.jvolgeores.2009.06.012.
Forasiepi, A.M., Martinelli, A.G., De la Fuente, M.S., Dieguez, S., Bond, M., 2011. Paleontology and stratigraphy of the Aisol Formation (Neogene), San Rafael, Mendoza. In: Cenozoic Geology of the Central Andes of Argentina. SCS Publisher, Salta, pp. 135–154. Salfity and Marquillas.
Fuentes, F., Horton, B.K., Starck, D., Boll, A., 2016. Structure and tectonic evolution of hybrid thick-and thin-skinned systems in the Malargüe fold–thrust belt, Neuquén basin, Argentina. Geol. Mag. 153 (5–6), 1066–1084. https://doi.org/10.1017/S0016756816000583.
García, V.H., Casa, A.L., 2015. Quaternary tectonics and seismic potential of the Andean retrowedge at 33–34° S. Geological Society, London, Special Publications 399 (1), 311–327. https://doi.org/10.1144/SP399.11.
García, V.H., Toural Dapoza, R., Giambiagi, L., Moreiras, S., 2015. Evolución tectónica y del relieve durante el Cuaternario en las Huayquerias del este (34°S), Cerrilladas Pedemontanas, Mendoza. XVI Reunión de Tectónica, Resúmenes, pp. 192–193.
González Bonorino, F., 1950. Algunos problemas geológicos de las Sierras Pampeanas. Rev. Asoc. Geol. Argent. 5 (3), 6–110.
González Díaz, E.F., 1972. Descripción geológica de la hoja 27d, San Rafael, vol. 132. Servicio Nacional Minero Geológico, Boletín, pp. 1–127 (Buenos Aires).
Havskov, J., Voss, P.H., Ottemöller, L., 2020. Seismological Observatory Software: 30 Yr of SEISAN. Seismol Res. Lett. 91 (3), 1846–1852. https://doi.org/10.1785/0220190313.
Hayes, G.P., Moore, G.L., Portner, D.E., Hearne, M., Flamme, H., Furtney, M., Smoczyk, G.M., 2018. Slab2, a comprehensive subduction zone geometry model. Science 362 (6410), 58–61. https://doi.org/10.1126/science.aat4723.
Heck, B., Seitz, K., 2007. A comparison of the tesseroid, prism and point-mass approaches for mass reductions in gravity field modelling. J. Geodes. 81 (2), 121–136.
Heit, B., Yuan, X., Bianchi, M., Sodoudi, F., Kind, R., 2008. Crustal thickness estimation beneath the southern central Andes at 30 S and 36 S from S wave receiver function analysis. Geophys. J. Int. 174 (1), 249–254. https://doi.org/10.1111/j.1365-246X.2008.03780.x.
Henry, L.C., Isbell, J.L., Limarino, C.O., 2014. The late Paleozoic El Imperial Formation, western Argentina: Glacial to post-glacial transition and stratigraphic correlations with arc-related basins in southwestern Gondwana. Gondwana Res. 25 (4), 1380–1395. https://doi.org/10.1016/j.gr.2012.08.023.
Introcaso, A., Lion, A., Ramos, V., 1987. La estructura profunda de las Sierras de Córdoba. Rev. Asoc. Geol. Argent. 42 (1–2), 177–187.
International Seismological Centre, 2019. ISC-GEM Earthquake Catalogue. https://doi.org/10.31905/d808b825.
Jordan, T.E., Allmendinger, R.W., 1986. The Sierras Pampeanas of Argentina; a modern analogue of Rocky Mountain foreland deformation. Am. J. Sci. 286 (10), 737–764.
Kay, S.M., Burns, W.M., Copeland, P., Mancilla, O., 2006. Upper Cretaceous to Holocene magmatism and evidence for transient Miocene shallowing of the Andean subduction zone under the northern Neuquén Basin. Spec. Pap. Geol. Soc. Am. 407, 19. https://doi.org/10.1130/2006.2407(02.
Kleiman, L.E., Japas, M.S., 2005. The Upper Choiyoi Volcanism, San Rafael, Mendoza, Argentina: A Transitional Sequence Emplaced under Changing Geodynamic Conditions. Abstracts Gondwana XII. Academia Nacional de Ciencias, Mendoza.
Lienert, B.R., Havskov, J., 1995. A computer program for locating earthquakes both locally and globally. Seismol Res. Lett. 66 (5), 26–36.
Llambías, E.J., Kleiman, L.E., Salvarredi, J.A., 1993. El magmatismo gondwánico. In: Ramos (Ed.), Geología de la provincia de Mendoza: XII Congreso Geologico Argentino Relatorio, pp. 53–64.
Lomax, A., Virieux, J., Volant, P., Berge-Thierry, C., 2000. Probabilistic earthquake location in 3D and layered models. In: Advances in Seismic Event Location. Springer, Dordrecht, pp. 101–134.
Lucero, C., Paredes, J., 1999. Fallamiento rumbo-deslizante en la falla Aisol, Bloque de San Rafael, Mendoza. XIV Congreso Geológico Argentino, Actas, pp. 263–266 (Salta).
Lupari, M.N., Spagnotto, S.L., Nacif, S.V., Yacante, G., García, H.P.A., Lince-Klinger, F., et al., 2015. Sismicidad localizada en la zona del Bloque San Rafael, Argentina. Rev. Mex. Ciencias Geol. 32 (2), 190–202.
MacLeod, I.N., Ellis, R.G., 2016. Quantitative magnetization vector inversion. ASEG Extended Abstracts 2016 (1), 1–6. https://doi.org/10.1071/ASEG2016ab115.
May, V.R., Chivas, A.R., Dosseto, A., Honda, M., Matchan, E.L., Phillips, D., Price, D.M., 2018. Quaternary volcanic evolution in the continental back-arc of southern Mendoza, Argentina. J. S. Am. Earth Sci. 84, 88–103. https://doi.org/10.1016/j.jsames.2018.02.007.
Meigs, A., Krugh, W.C., Schiffman, C., Vergés, J., Ramos, V.A., 2006. Refolding of thin-skinned thrust sheets by active basement-involved thrust faults in the eastern Precordillera of western Argentina. Rev. Asoc. Geol. Argent. 61 (4), 589–603.
Messager, G., Nivière, B., Lacan, P., Hervouët, Y., Xavier, J.P., 2014. Plio-Quaternary thin-skinned tectonics along the crustal front flexure of the southern Central Andes: A record of the regional stress regime or of local tectonic-driven gravitational processes? Int. J. Earth Sci. 103 (3), 929–951. https://doi.org/10.1007/S00531-013-0983-4/TABLES/3.
Mpodozis, C., Kay, S.M., 1990. Provincias magmáticas ácidas y evolución tectónica de Gondwana: Andes chilenos (28-31 S). Andean Geol. 17 (2), 153–180.
Morales Volosín, M.S., Prezzi, C., Risso, C., 2022. Relationships between Payenia volcanism and deep-seated structural controls: Insights from geophysical methods at Nevado volcanic field, Mendoza, Argentina. J. S. Am. Earth Sci. 116, 103779 https://doi.org/10.1016/j.jsames.2022.103779.
Müller, R.D., Seton, M., Zahirovic, S., Williams, S.E., Matthews, K.J., Wright, N.M., Shephard, G.E., Maloney, K.T., Barnett-Moore, N., Hosseinpour, M., Bower, D.J., Cannon, J., 2016. Ocean Basin Evolution and Global-Scale Plate Reorganization Events Since Pangea Breakup. Annu. Rev. Earth Planet Sci. 44 (1), 107–138. https://doi.org/10.1146/annurev-earth-060115-012211.
Nacif, S., Triep, E.G., Spagnotto, S.L., Aragon, E., Furlani, R., Álvarez, O., 2015. The flat to normal subduction transition study to obtain the Nazca plate morphology using high resolution seismicity data from the Nazca plate in Central Chile. Tectonophysics 657, 102–112. https://doi.org/10.1016/j.tecto.2015.06.027.
Neilson, H., 2007. Evolution of the Santa Isabel Escarpment, Southern Mendoza, Argentina. Unpublished Honors Dissertation. Dalhousie University, Halifax, Nova Scotia, Canada.
Nullo, F.E., Stephens, G., Combina, A., Dimieri, L., Baldauf, P., Bouza, P., Zanettini, J.C., 2005. Hoja Geológica 3569-III/3572IV, Malargüe, provincia de Mendoza. Servicio Geológico Minero Argentino, vol. 346. Instituto de Geología y Recursos Minerales, Boletín, Buenos Aires, p. 85.
Olivar, J., Nacif, S., García, H., Fennell, L., Heit, B., Folguera, A., 2022. Controls on crustal seismicity segmentation on a local scale in the Southern Central Andes. J. S. Am. Earth Sci. 116, 103778 https://doi.org/10.1016/j.jsames.2022.103778.
Pavlis, N.K., Holmes, S.A., Kenyon, S.C., Factor, J.K., 2008. An Earth Gravitational Model to Degree 2160: EGM2008. General Assembly of the European Geosciences Union, Vienna, Austria.
Pavlis, N.K., Holmes, S.A., Kenyon, S.C., Factor, J.K., 2012. The development and evaluation of the Earth Gravitational Model 2008 (EGM2008). J. Geophys. Res. Solid Earth 117 (B4). https://doi.org/10.1029/2011JB008916.
Peñalva, M.L., Velez, M.L., 2005. Análisis estructural de la deformación cenozoica, sector sur Bloque de San Rafael, Mendoza (34º 50′- 35º S, 68º 27′- 68º 37′ O). XVI Congreso Geológico Argentino, Actas, Artículo Nº 528, 4 (La Plata).
Quidelleur, X., Carlut, J., Tchilinguirian, P., Germa, A., Gillot, P.Y., 2009. Paleomagnetic directions from mid-latitude sites in the southern hemisphere (Argentina): contribution to time averaged field models. Phys. Earth Planet. In. 172 (3–4), 199–209. https://doi.org/10.1016/j.pepi.2008.09.012.
Ramos, V.A., Folguera, A., 2005. Tectonic evolution of the Andes of Neuquén: constraints derived from the magmatic arc and foreland deformation. Geological Society, London, Special Publications 252 (1), 15–35. https://doi.org/10.1144/GSL.SP.2005.252.01.02.
Ramos, V.A., Folguera, A., 2011. Payenia volcanic province in the Southern Andes: An appraisal of an exceptional Quaternary tectonic setting. J. Volcanol. Geoth. Res. 201 (1–4), 53–64. https://doi.org/10.1016/j.jvolgeores.2010.09.008.
Ramos, V.A., Kay, S.M., 2006. Overview of the tectonic evolution of the southern Central Andes of Mendoza and Neuquén (35–39 S latitude). In: Kay & Ramos (Ed.), Evolution of an Andean Margin: A Tectonic and Magmatic View from the Andes to the Neuquén Basin (35°–39°S Lat). Geological Society of America, p. 342. https://doi.org/10.1130/2006.2407(01. Special Paper no. 407.
Ramos, V.A., Dallmeyer, R.D., Vujovich, G., 1998. Time constraints on the Early Palaeozoic docking of the Precordillera, central Argentina. Geological Society, London, Special Publications 142 (1), 143–158. https://doi.org/10.1144/GSL.SP.1998.142.01.08.
Ramos, V.A., Cristallini, E.O., Pérez, D.J., 2002. The Pampean flat-slab of the Central Andes. J. S. Am. Earth Sci. 15 (1), 59–78. https://doi.org/10.1016/S0895-9811(02)00006-8.
Ramos, V.A., Litvak, V.D., Folguera, A., Spagnuolo, M., 2014. An Andean tectonic cycle: From crustal thickening to extension in a thin crust (34–37 SL). Geosci. Front. 5 (3), 351–367. https://doi.org/10.1016/j.gsf.2013.12.009.
Richarte, D., Lupari, M., Pesce, A., Nacif, S., Gimenez, M., 2018. 3-D crustal-scale gravity model of the San Rafael Block and Payenia volcanic province in Mendoza, Argentina. Geosci. Front. 9 (1), 239–248. https://doi.org/10.1016/j.gsf.2017.03.004.
Rocha-Campos, A.C., Basei, M.A.S., Nutman, A.P., Santos, P.D., 2006. SHRIMP U-Pb zircon geochronological calibration of the late Paleozoic supersequence, Paraná Basin, Brazil. April. In: V South American Symposium on *Isotope Geology*. Idea Gráfica, Buenos Aires, pp. 298–301.
Rocha-Campos, A.C., Basei, M.A., Nutman, A.P., Kleiman, L.E., Varela, R., Llambias, E., et al., 2011. 30 million years of Permian volcanism recorded in the Choiyoi igneous

province (W Argentina) and their source for younger ash fall deposits in the Paraná Basin: SHRIMP U–Pb zircon geochronology evidence. Gondwana Res. 19 (2), 509–523. https://doi.org/10.1016/j.gr.2010.07.003.

Sagripanti, L., Rojas Vera, E.A., Gianni, G.M., Folguera, A., Harvey, J.E., Farías, M., Ramos, V.A., 2015. Neotectonic reactivation of the western section of the Malargüe fold and thrust belt (Tromen volcanic plateau, Southern Central Andes). Geomorphology 232, 164–181. https://doi.org/10.1016/J.GEOMORPH.2014.12.022.

SEGEMAR, 2021. Catálogo de Datos Abiertos Geoespaciales, Deformaciones Cuaternarias 250k. Sistema de Información Geológica Ambiental Minera (SIGAM).

Sepúlveda, E., Carpio, F., Regairaz, M., Zárate, M., Zanettini, J., 2007a. Hoja Geológica 3569-II, San Rafael, provincia de Mendoza. Servicio Geológico Minero Argentino, vol. 321. Instituto de Geología y Recursos Minerales, Boletín, Buenos Aires segunda edición revisada, 59pp.

Sepúlveda, E., Bermúdez, A., Bordonaro, O., Delpino, D., 2007b. Hoja Geológica 3569-IV, Embalse El Nihuil, provincia de Mendoza. Servicio Geológico Minero Argentino, vol. 268. Instituto de Geología y Recursos Minerales, Boletín, Buenos Aires segunda edición revisada, 52pp.

Smithson, S.B., Brewer, J., Kaufman, S., Oliver, J., Hurich, C., 1978. Nature of the Wind River thrust, Wyoming, from COCORP deep-reflection data and from gravity data. Geology 6 (11), 648–652.

Sruoga, P., Etcheverría, M., Folguera, A., Repol, D., Zanettini, J.C., 2005. Hoja Geológica 3569-I, Volcán Maipo. Provincia de Mendoza. Servicio Geológico Minero Argentino, vol. 290. Instituto de Geología y Recursos Minerales, Boletín, Buenos Aires, p. 92.

Stone, D.S., Schmidt, C.J., Chase, R.B., Erslev, E.A., 1993. Basement-involved Thrust-Generated Folds as Seismically Imaged in the Subsurface of the Central Rocky Mountain Foreland. Special papers-Geological Society of America, p. 271.

Tarantola, A., Valette, B., 1982. Generalized nonlinear inverse problems solved using the least squares criterion. Rev. Geophys. 20 (2), 219. https://doi.org/10.1029/RG020i002p00219.

Tickyj, H., Cingolani, C.A., Varela, R., Chemale, F., 2017. Low-grade metamorphic conditions and isotopic age constraints of the La Horqueta pre-Carboniferous sequence, Argentinian San Rafael Block. In: Cingolani (Ed.), Pre-carboniferous Evolution of the San Rafael Block. Springer, Argentina, pp. 137–159 (Cham).

Turienzo, M., Dimieri, L., Frisicale, C., Araujo, V., Sánchez, N., 2012. Cenozoic structural evolution of the Argentinean Andes at 34° 40'S: A close relationship between thick and thin-skinned deformation. Andean Geol. 39 (2), 317–357. https://doi.org/10.5027/andgeoV39n2-a07.

Uieda, L., Barbosa, V.C., 2017. Fast nonlinear gravity inversion in spherical coordinates with application to the South American Moho. Geophys. J. Int. 208 (1), 162–176. https://doi.org/10.1093/gji/ggw390.

Uieda, L., Ussami, N., Braitenberg, C.F., 2010. Computation of the gravity gradient tensor due to topographic masses using tesseroids. Eos Trans. AGU 91 (26).

Vicente, J., Spagnotto, S.L., Dávila, F.M., 2022. Crustal focal mechanisms in the NW sierras de cordoba, and connections with mio-pliocene basement thrusting of the easternmost Sierras Pampeanas, south-Central Andes. J. S. Am. Earth Sci. 120, 104074 https://doi.org/10.1016/j.jsames.2022.104074.

Yonkee, W.A., Weil, A.B., 2015. Tectonic evolution of the Sevier and Laramide belts within the North American Cordillera orogenic system. Earth Sci. Rev. 150, 531–593. https://doi.org/10.1016/J.EARSCIREV.2015.08.001.

References from the appendices

Moser, T.J., Van Eck, T., Nolet, G., 1992. Hypocenter determination in strongly heterogeneous earth models using the shortest path method. J. Geophys. Res. Solid Earth 97 (B5), 6563–6572. https://doi.org/10.1029/91JB03176.